

Supplementary Figure S1: Rate of ice elevation changes in Alaska. The thin black line corresponds to our new ice inventory. Areas where no reliable elevation changes could be measured are denoted in white. (a) Eastern part of the Alaska Range; (b) Central part of the Alaska Range; (c) Western part of the Alaska Range; (d) Mt Katmai National Park icefields in the Alaska Peninsula; (e) Kenai Peninsula; (f) Wrangell and St Elias Mountains; (g) Coast Mountains. Elevation changes in the Western Chugach Mountains are shown in Figure 2 of the article.

Figure S1a

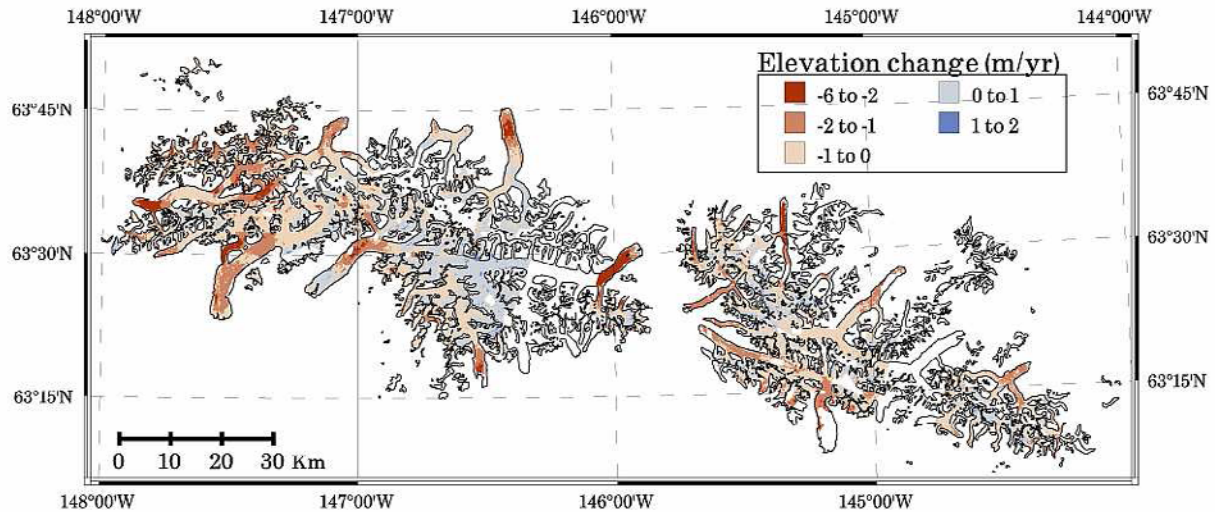


Figure S1b

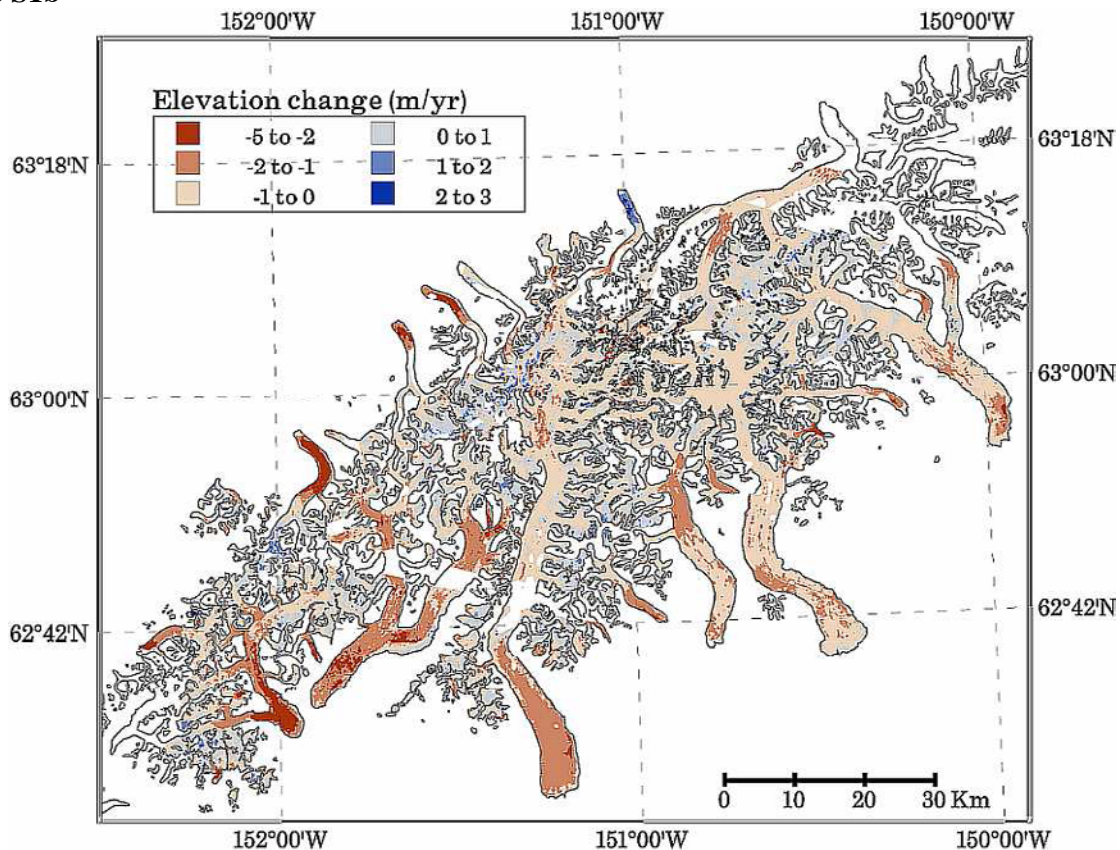


Figure S1c

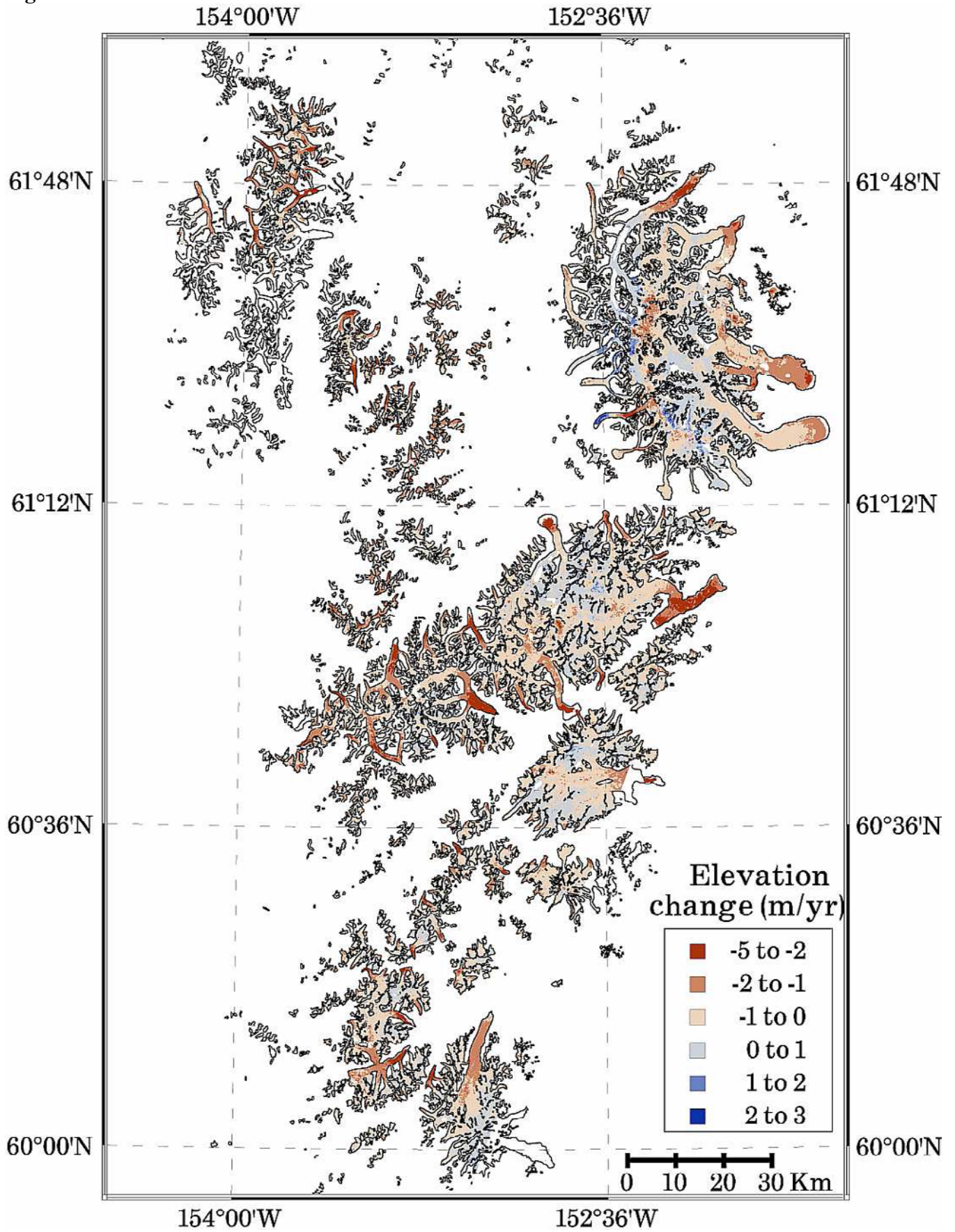


Figure S1d

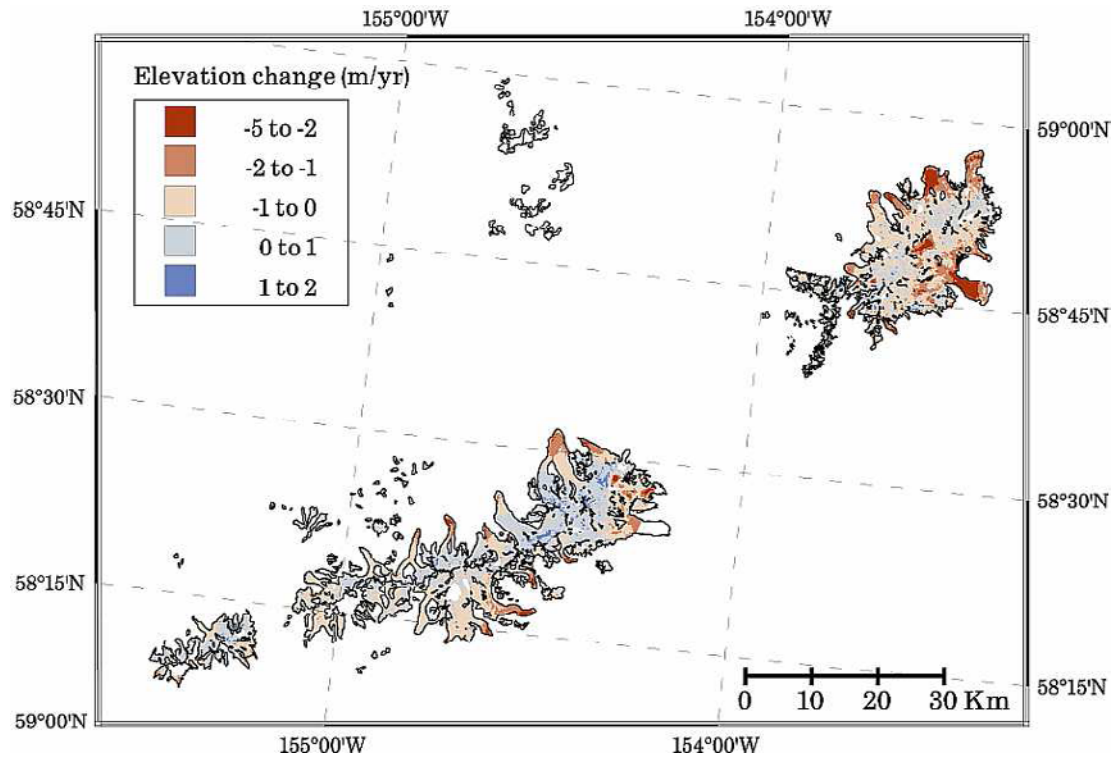


Figure S1e

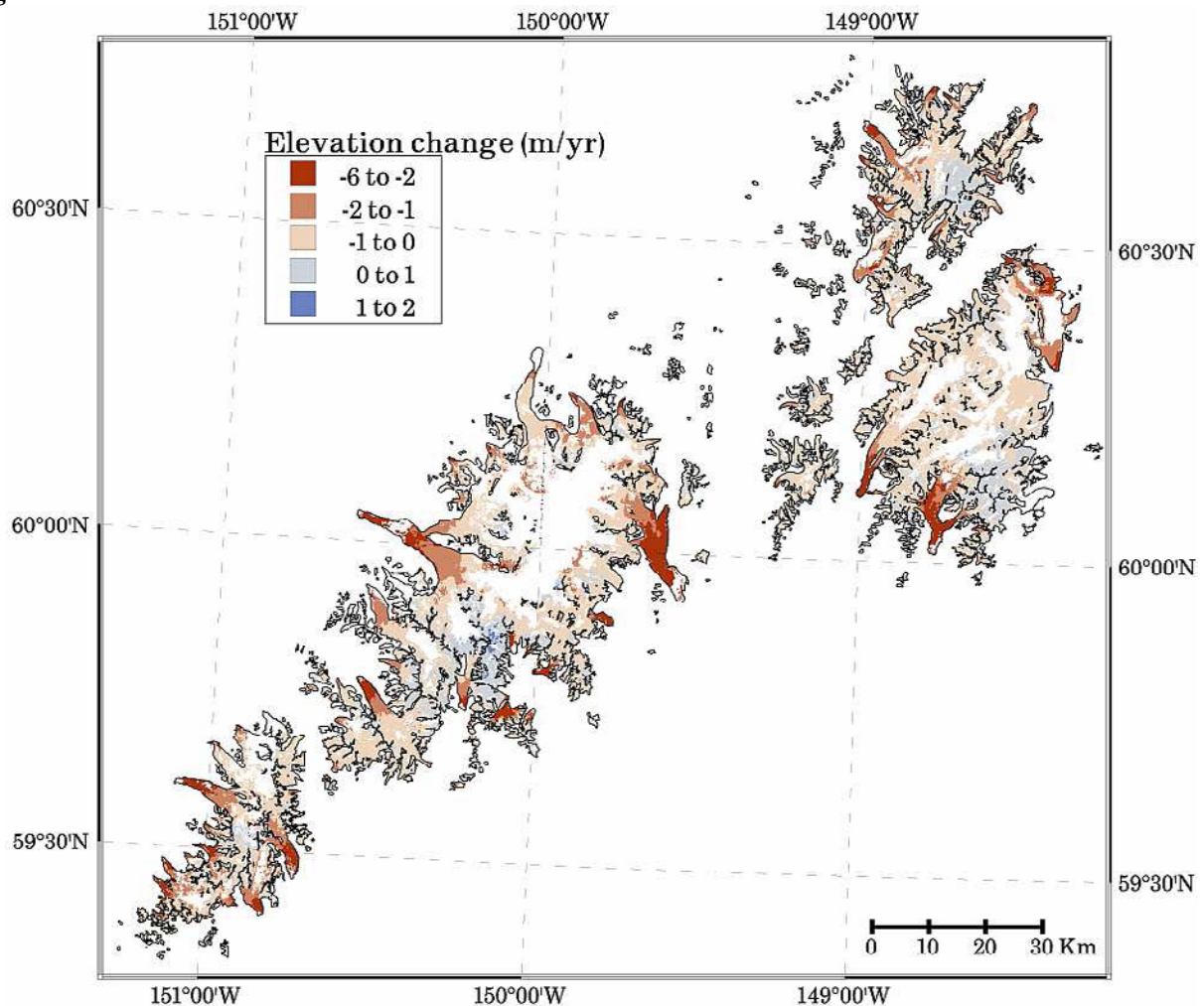


Figure S1f

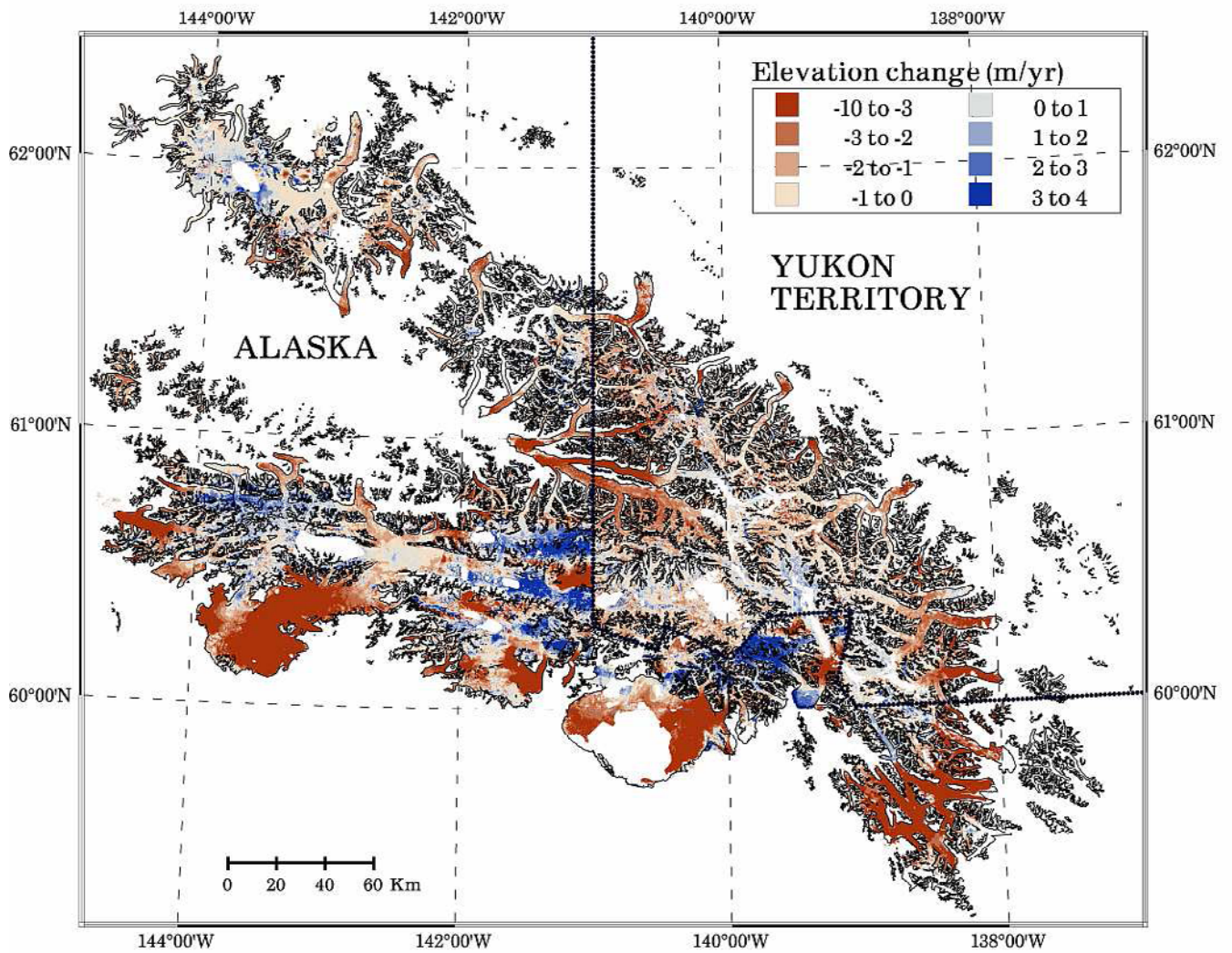
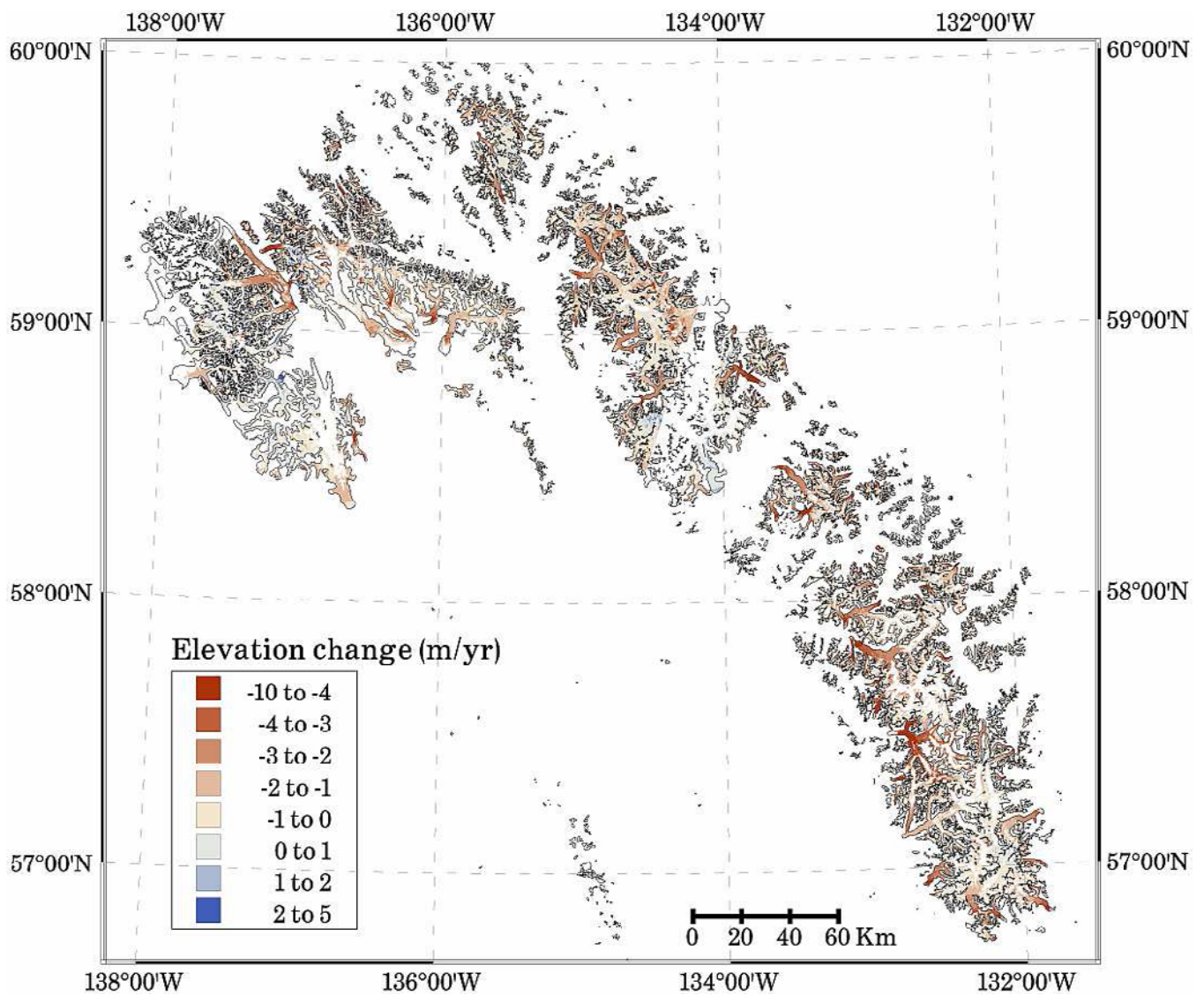


Figure S1g



Supplementary Figure S2: Hypsometry and rate of ice elevation change versus elevation in Alaska. (a) Eastern part of the Alaska Range; (b) Central part of the Alaska Range; (c) Western part of the Alaska Range; (d) Mt Katmai National Park icefields in the Alaska Peninsula; (e) Kenai Peninsula; (f) Wrangell and St Elias Mountains with elevation changes for Bering Glacier System shown with grey triangles; (g) Coast Mountains. Elevation changes in the Western Chugach Mountains are shown in Figure 2 of the article. The different sub-regions of the Alaska Range are located in Figure 1.

Figure S2a

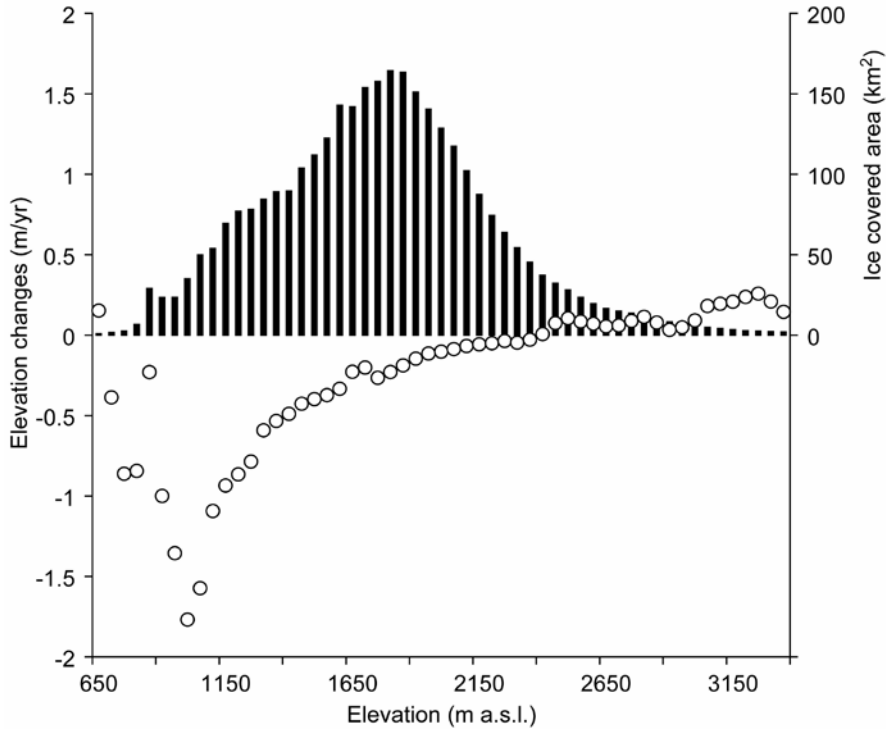


Figure S2b

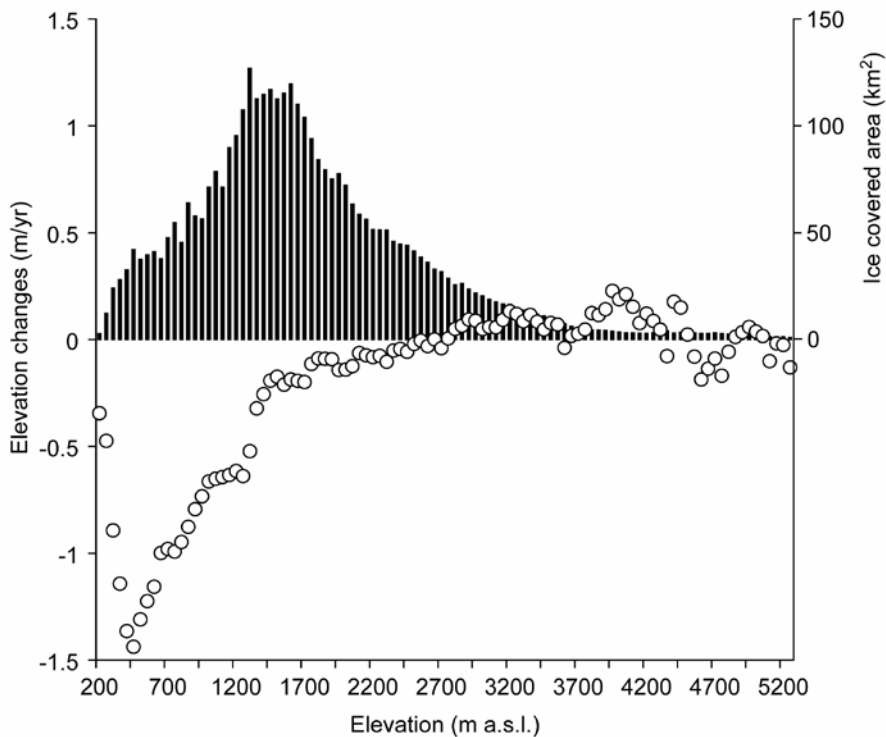


Figure S2c

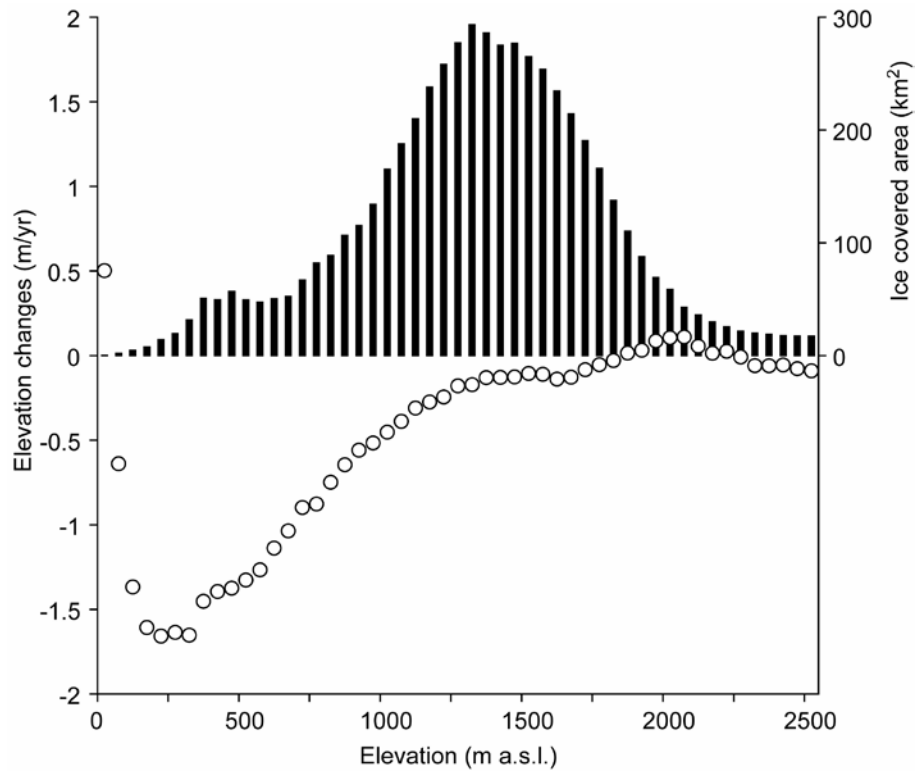


Figure S2d

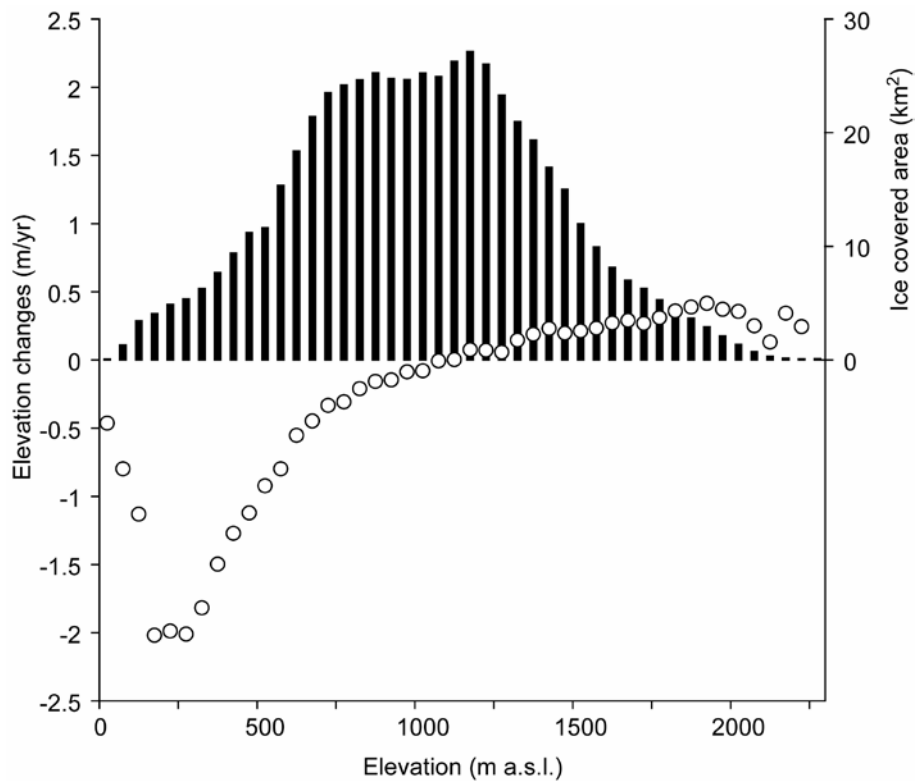


Figure S2e

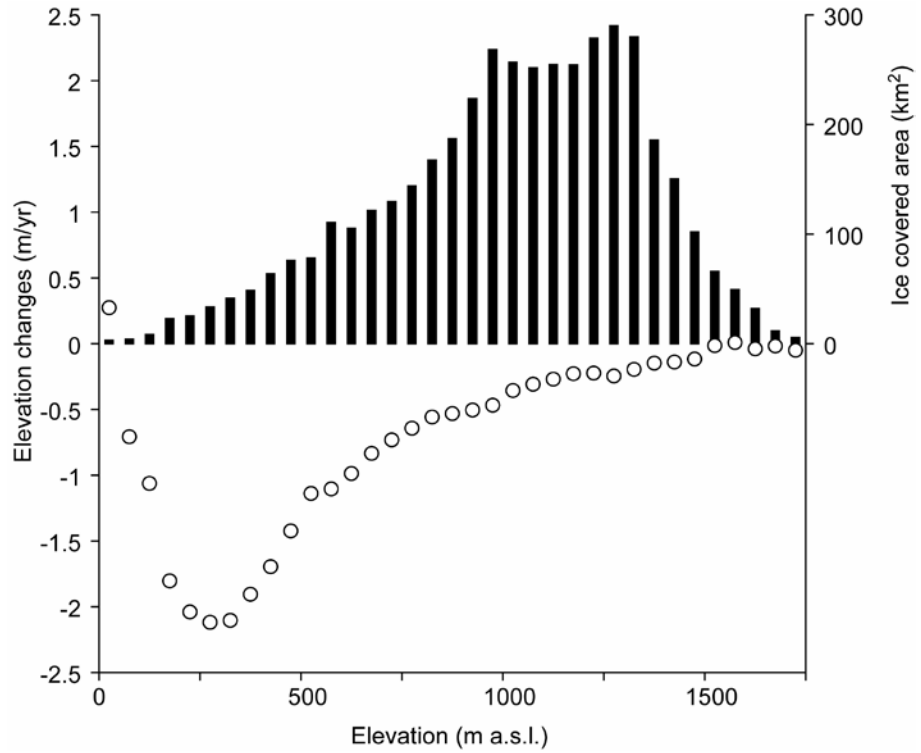


Figure S2f

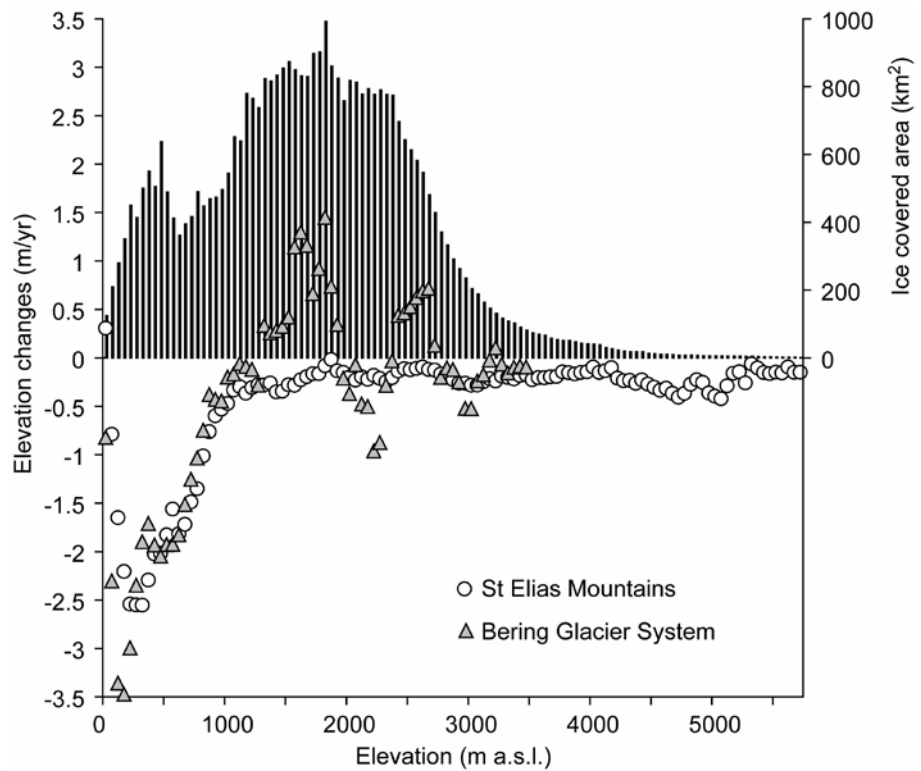
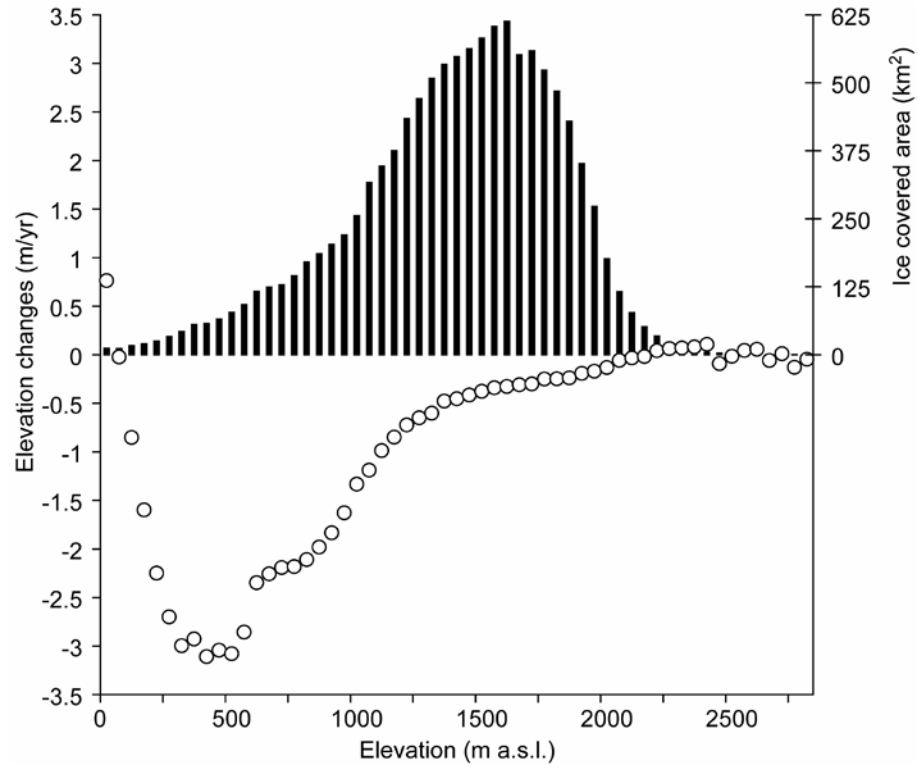
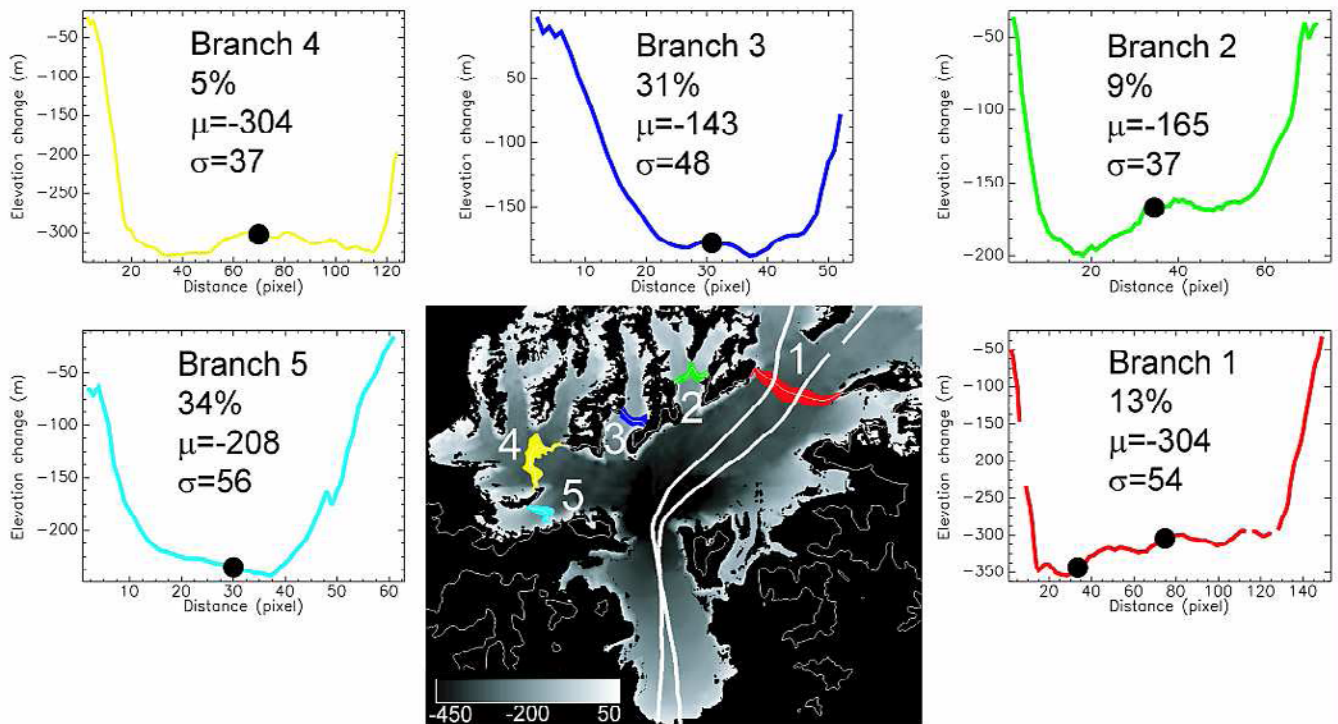


Figure S2g



Supplementary Figure S3: Elevation changes during 1957-2007 for five different branches of Columbia Glacier. The central panel is the elevation change map with the [671 m, 701 m] altitude band (from the USGS DEM) coloured for five branches (labelled from 1 to 5); the thick white lines locate the laser profiles². The five other panels show the transverse profiles of elevation changes along the 686 m contour. On each panel, a black dot shows the elevation change that would have been sampled by an airborne laser following the glacier branch centreline (except for branch 1 where we plot the actual location of the two laser profiles used in Arendt *et al.*²). For each branch, the relative difference (in percent) between the centreline and the mean transverse elevation change is given. We also indicate on each panel the mean (μ) and standard deviation (σ) of the elevation differences (in meters) for the [671 m, 701 m] altitude band.



Supplementary Table S1: Source of uncertainties at the 1-pixel level in our estimate of ice volume changes. Other sources of systematic errors (e.g. seasonal variations in ice elevation, floating contours, uplift of the solid earth) are discussed in the Supplementary Note.

Error Component	Error (m)	Reference
Map elevations (ablation area)	± 15	14
Map elevations (accumulation area)	± 45	31
ASTER elevations	± 15	12
Spot5 elevations	± 10	13
Ice inventory	$\pm 10\%$	This study
Map date	± 3.5 yr	14

Supplementary Table S2: Statistics for the elevation differences (Satellite_DEM – Map_DEM) on the ice-free terrain surrounding the different glaciated regions. Absolute elevation differences larger than 100 m were considered as outliers and excluded from the statistics. The standard deviation (Std dev) is large but does not account for the error reduction which occurs by averaging elevation changes over large regions. We calculated a standard error (SE_z) after reducing our sample size to account for spatial autocorrelation in the sequential DEM³². The decorrelation length is on average 500 m.

Region	Mean (m)	Std dev (m)	Area (km ²)	SE _z (m)
Alaska Range - East	-0.4	23.5	5860	0.06
Alaska Range - Central	5.0	26.1	5963	0.06
Alaska Range - West	-1.3	27.1	17984	0.04
Alaska Peninsula	-1.6	21.9	2828	0.07
Kenai Peninsula	-3.9	23.2	4529	0.06
Western Chugach Mts	-1.3	22.8	20445	0.03
St Elias and Wrangell Mts	1.3	23.7	26092	0.02
Coast Mts	-0.35	29.7	27773	0.03
Area-weighted Mean	-0.5	25.6		0.04

Supplementary Table S3: Comparison of field-based and DEM-derived mass balances (denoted B) for Gulkana and Wolverine glaciers. The field-based mass balances are those reported in Josberger *et al.*¹⁹. They are under revision by the USGS (O'Neel, personal communication, 2009).

Glacier	Area km ²	Field period	B_FIELD m yr ⁻¹ w.e.	DEM period	B_DEM m yr ⁻¹ w.e.
Gulkana	20	1966-2005	-0.40	1954-2006	-0.39 ± 0.13
Wolverine	18.5	1966-2004	-0.37	1950-2007	-0.41 ± 0.12

Supplementary Table S4: Over-estimation of ice loss by laser altimetry for ten large glaciers in Alaska. Our sample includes glaciers that experienced ice losses larger than $0.1 \text{ km}^3 \text{ yr}^{-1}$ in the early period (1950s to 1995) studied by Arendt *et al.*² (their Table S1) and whose outlines were available on the National Snow and Ice Data Center website. Taken together, these ten glaciers account for half of the total ice loss measured by Arendt *et al.*² on 67 glaciers. The glacier area is based on the Arendt *et al.*² outlines and may differ from the real glacier extent, in particular for Bering Glacier³³. ΔV_{DEM} corresponds to the actual ice loss measured from sequential DEM. $\Delta V_{\text{SIMU-LASER}}$ corresponds to a simulated ice loss based on elevation changes extracted from sequential DEM solely where Arendt *et al.*²’s laser profiles crossed the USGS map contour lines. The large overestimation of the ice loss for Nabesna Glacier is due to the fact that laser profiles were restricted to low elevations and did not sample some large regions of ice gain at high elevations. ΔV_{UAF} is constructed from Arendt *et al.*² (their Table S1) by time-weighting their ice loss during the early and recent period, assuming that the loss for the recent period (reported for seven glaciers identified by an asterisk) are also valid after 2001. The last column indicates (in percent) the relative difference between $\Delta V_{\text{SIMU-LASER}}$ and ΔV_{DEM} . Positive values thus correspond to a percentage of overestimation of the ice loss by $\Delta V_{\text{SIMU-LASER}}$.

Glacier	Area km ²	ΔV_{DEM} km ³ yr ⁻¹ w.e.	$\Delta V_{\text{SIMU-LASER}}$ km ³ yr ⁻¹ w.e.	ΔV_{UAF} km ³ yr ⁻¹ w.e.	$\frac{\Delta V_{\text{SIMU-LASER}} - \Delta V_{\text{DEM}}}{\Delta V_{\text{DEM}}} \times 100$
Bering*	2,190	-2.45	-3.09	-2.87	26.2
Columbia*	1,090	-2.43	-3.09	-3.07	27.2
Nabesna	1,040	-0.04	-0.08		95.0
Baird*	523	-0.25	-0.24	-0.20	-5.6
Le Conte*	454	-0.22	-0.29	-0.37	31.8
Tazlina*	433	-0.31	-0.33	-0.30	7.3
Double*	232	-0.07	-0.09	-0.13	16.0
Bear	229	-0.21	-0.18		-15.2
Tanaina*	168	-0.10	-0.09	-0.13	-6.8
Valdez	164	-0.16	-0.18		13.7
Total 10 Glaciers	6,523	-6.23	-7.65		22.7
Total 7 glaciers	5,090	-5.83	-7.22	-7.04	

Supplementary Table S5: Spot5-HRS and ASTER satellite data used in each mountain range and their validation/calibration against ICESat data. Dates are given as YYYY-MM-DD. Spot5-HRS product Id corresponds to those used by the SPIRIT project (<http://www.spotimage.fr/web/en/1587-international-polar-year.php>). When different images from one ASTER strip have been used, only the Id of the northernmost image has been given. We also indicate the ICESat laser periods used to calibrate the satellite DEMs, the mean, standard deviation of the elevation differences between the DEMs (before calibration) and ICESat profiles (N is the number of points where the comparison has been computed). The last two columns are the two parameters (see Methods) of a linear model used to correct the elevation bias of each satellite DEM.

Sensor	Date	Product Id	ICESat	Mean (m)	St dev. (m)	N	α (m/1000m)	β (m)
<i>Alaska Range – East</i>								
ASTER	2003-07-08	SC:AST_L1A.003:2015245388	2A	-5.3	11.3	536	7.6	-15.8
ASTER	2004-06-28	SC:AST_L1A.003:2024895667	2C	-13.3	12.1	491	-6.0	-6.8
ASTER	2005-08-09	SC:AST_L1A.003:2030399469	3D	-2.5	15.7	261	0.2	-2.8
ASTER	2006-07-20	SC:AST_L1A.003:2035265461	3G	-9.5	15.9	480	2.7	-14.2
<i>Alaska Range – Central</i>								
ASTER	2001-09-27	SC:AST_L1A.003:2004406103	2A	-14.0	15.0	802	0.6	-14.6
ASTER	2003-09-10	SC:AST_L1A.003:2017111646	2A	-13.9	12.9	579	0.5	-14.7
ASTER	2005-05-08	SC:AST_L1A.003:2028948307	3G	-11.4	18.5	1228	2.4	-14.1
<i>Alaska Range – West</i>								
ASTER	2003-05-03	SC:AST_L1A.003:2013305676	2A	11.0	19.3	1826	4.4	6.7
ASTER	2003-09-08	SC:AST_L1A.003:2017088192	2A	-2.6	13.5	867	4.8	-6.9
ASTER	2005-05-08	SC:AST_L1A.003:2028948311	3D	-9.6	16.6	2605	5.0	-14.6
ASTER	2006-03-01	SC:AST_L1A.003:2033287700	3G	-1.3	18.2	1533	7.5	-8.8
ASTER	2008-10-16	SC:AST_L1A.003:2066900536	3G	-12.0	18.1	1569	4.0	-15.3
<i>Alaska Peninsula (Mt Katmai National Park)</i>								
ASTER	2002-10-09	SC:AST_L1A.003:2008676413	2A	-0.9	15.5	293	0.4	-1.8
ASTER	2004-07-08	SC:AST_L1A.003:2024993226	3A	-12.2	10.8	1051	-5.9	-9.1
<i>Kenai Peninsula</i>								
Spot5-HRS	2007-07-16	GES 08-027	3I	-2.9	7.8	568	-0.3	-2.6
<i>Western Chugach Mountains</i>								
ASTER	2003-07-08	SC:AST_L1A.003:2015245390	2A	-9.8	13.5	1176	5.3	-16.6
Spot5-HRS	2007-07-16	GES 08-027	3I	-2.9	7.8	568	-0.3	-2.6
Spot5-HRS	2007-09-22	GES 08-028	3I	-0.5	7.4	486	-2.5	2.3
<i>St Elias and Wrangell Mountains</i>								
ASTER	2003-08-08	SC:AST_L1A.003:2015906911	2A	-12.9	12.6	998	-3.2	-9.5
ASTER	2004-05-04	SC:AST_L1A.003:2023060288	2C	-9.4	12.4	449	2.2	-11.7
ASTER	2004-07-16	SC:AST_L1A.003:2025074017	3A	-19.9	11.9	650	0.3	-20.4
ASTER	2004-08-03	SC:AST_L1A.003:2025207562	3A	-1.7	14.2	2208	0.3	-2.3
ASTER	2004-08-10	SC:AST_L1A.003:2025302220	3A	-2.2	13.1	335	3.6	-6.1
ASTER	2004-08-17	SC:AST_L1A.003:2025331799	3A	-13.4	16.9	743	3.8	-18.9
ASTER	2006-05-21	SC:AST_L1A.003:2034308352	3F	-9.1	17.2	556	-2.9	-4.3
ASTER	2006-08-07	SC:AST_L1A.003:2035903767	3G	-21.5	16.8	1995	0.1	-21.7
ASTER	2006-08-09	SC:AST_L1A.003:2035969681	3G	-7.8	15.3	338	0.8	-9.7
Spot5-HRS	2006-09-13	GES 08-040	3G	8.3	6.8	2458	-1.7	9.9
Spot5-HRS	2007-09-03	GES 08-029	3I	-3.0	7.5	870	0.2	-3.2
Spot5-HRS	2007-09-13	GES 07-044	3I	5.4	6.7	1376	0.1	5.4
<i>Coast Mountains (Glacier Bay, Juneau and Stikine icefields)</i>								
ASTER	2004-08-23	SC:AST_L1A.003:2025854043	3A	-6.1	13.7	761	-1.4	-4.4
ASTER	2005-08-10	SC:AST_L1A.003:2030408819	3D	-9.8	10.9	915	-4.5	-4.6
Spot5-HRS	2008-05-26	SPI 09-014	3I	-3.6	6.5	420	1.5	-4.7
Spot5-HRS	2008-05-27	SPI 09-013	3I	5.5	5.9	366	-1.4	7.3
Spot5-HRS	2008-07-02	SPI 09-012	3I	2.1	7.9	222	-1.0	3.4

Supplementary Notes: error analysis

1. Uncertainty for our total ice loss estimate

Errors in surveyed areas

Our formal error analysis is similar to the one used previously to compare laser altimetry to map elevation contour lines¹⁴. Random errors are listed in Supplementary Table S3. In each ice-covered area, these different elevation errors were summed quadratically and divided by the square root of the number of map elevation contour lines. By adjusting the old and recent elevation dataset (map and satellite DEMs) to a common reference (ICESat laser profiles), we minimized systematic elevation errors due to poor map geodetic control. A $\pm 10\%$ error was also included for the total ice-covered area. This value represents approximately the scatter between the different published estimates of glaciated area in Alaska^{2,9,11}.

Errors due to extrapolation to unsurveyed areas (regional extrapolation)

For unsurveyed areas (27% of the total ice-covered area), we assumed that errors doubled those calculated on surveyed areas.

In previous studies^{2,14}, some of the tidewater glaciers measured using laser altimetry have been deliberately excluded from the regional extrapolation because they had recently been subject to tidewater glacier dynamics. Here, we did not exclude those tidewater glaciers. To justify this choice and test the influence of including or excluding tidewater glaciers in the regional extrapolation, we examine the mass loss of the Western Chugach Mountains (WCM) when the marine-terminating Columbia Glacier (COL) is included or excluded in the extrapolation to unsurveyed areas of the WCM. The mass losses are respectively $5.81 \text{ km}^3/\text{yr}$ w.e. and $5.85 \text{ km}^3/\text{yr}$ w.e., differing by less than 1%. The inclusion of COL elevation changes for the extrapolation to unsurveyed areas of the WCM has thus a limited influence on the total regional ice loss. This is because (i) unsurveyed areas cover only 18% in the WCM (Table 1) and; (ii) unsurveyed areas mainly correspond to highest-elevation textureless regions (where DEMs derived from optical images contain large data gaps) that have a delayed and attenuated response to dramatic changes in frontal behaviour. Our analysis for COL in the WCM is a worst case scenario given that this glacier has experienced dramatic ice loss since 1980 and occupies over 10% of the total ice-covered area in the WCM. No other tidewater glacier in Alaska combines such a large relative area-coverage with rapid ice loss.

2. Other sources of errors

Some other sources of errors are not taken into account in this formal error analysis because they cannot be quantified.

Errors due to bed erosion

Changes in elevation over glaciers are assumed to arise from changes in glacier volume; we thus assume that changes in bed elevation due to sediment excavation and bed erosion over the period of study are small.

Errors due ice volume change below sea level

Our analysis also cannot account for gains or losses of ice below water for tidewater or lake-terminating glaciers. Because glacier ice is about 10% less dense than water, the corresponding overestimation of the sea level rise (for a retreating glacier) equals ~10% of the volume of ice previously below sea level¹⁴. It is not possible to correct this systematic error because of the lack of bathymetric data for most Alaskan fjords but its magnitude is small¹⁴.

Errors due the density of the material gain or loss

Total ice volume change in each region is converted to mass change assuming a constant density of 900 kg m^{-3} . This assumption may overestimate mass loss because it ignores the loss of firn that occurs from a rise of the equilibrium line altitude⁶. However, our observations reveal that about 80% of the ice loss took place in the ablation area, so errors that would result from this assumption are low.

Errors due floating contours in old maps

Floating of contours can lead to systematic errors in the accumulation area of old maps where aerial photographs lack sufficient contrast. There is no consensus on the magnitude of these errors and even its sign varies from one glacier to another. For example, Muskett *et al.*⁵ found that the Bagley Ice Valley was mapped 4 m too low and the Malaspina Glacier 6 m too high.

Errors due seasonal elevation changes

An underestimation of the thinning rates and thus, mass loss could arise because some of our DEMs were derived from satellite images not acquired at the end of the ablation season, leading generally to a glacier surface that is too high. We quantify this systematic error as

follows. First, we calculated the mean absolute temporal departure $|\delta t|$ from the end of the ablation season for all satellite DEMs. The end of the ablation season was assumed to be 15 September throughout Alaska^{20,34}. The area-weighted average $|\delta t|$ for our study is 0.14 year (51 days). $|\delta t|$ is multiplied by the mass balance annual amplitude for all Alaskan glaciers during recent years (2003-2007), 123 km³ w.e. according to an analysis of GRACE data²⁰. We calculate a systematic error of 17.2 km³ w.e. or 0.19 m w.e. (after dividing by the total area of Alaskan glaciers). The latter value accords with the 0.2 to 0.3 m w.e. glacier-wide ablation adjustment used by Cox and March³⁴ to account for a 40-60 days temporal difference between different DEMs of Gulkana Glacier. After dividing by the mean time separation between the two sets of DEMs (44 years), the systematic error is 0.4 km³/yr w.e. This is less than 1% of the total annual ice loss from all Alaskan glaciers. This error term is small in the present study because we consider a long time interval with large mass loss. If mass loss is examined from sequential DEMs over time periods of a decade or less, the fact that the DEMs are not acquired exactly at the end of the ablation season will substantially inflate the error estimate. The same problem also occurs for laser altimetry²².

Errors due to tectonics

Uplift rates as high as 32 mm/yr have been observed in South-East Alaska in response to the wastage of ice masses since the end of the little ice age³⁵. Over 40-50 years, the cumulative uplift can exceed 1 m and thus lead to systematic errors in the ice elevation changes and in our vertical adjustment of the map DEMs to ICESat data. Although the uplift is well-documented in South-East Alaska, to our knowledge, there is no uplift map covering all Alaskan ice masses to fully quantify this error. Furthermore, the maximum uplift rates are measured in the Glacier Bay region and rapidly decrease away from it. Following previous workers^{2,4}, this effect was not taken into account in our study.

Errors due to vegetation change

Although the height of the canopy can change over 40-50 years and thus bias our vertical adjustment of the map DEMs to ICESat data, we lack information to take this effect into account in our error analysis.

3. Uncertainty on the difference between our's and Arendt *et al.*² ice loss

Our ice losses and those of Arendt *et al.*² are characterized by relatively large uncertainties and, at first sight, are not statistically significantly different. However, an important source of errors comes from the old maps (see Table S1) and it is shared by both estimates. Here, by

calculating the volume loss of seven large glaciers using both methods (laser profiling vs. sequential DEM) and scaling the difference to all Alaskan glaciers, we demonstrate that both approaches differ.

First, we verify that we can reproduce (within 3.6%) the Arendt *et al.*²'s “early period” volume changes of 10 large glaciers (those in Table S4) using University of Alaska Fairbanks (UAF) data available from NSIDC. We have then used the same profile-to-glacier extrapolation scheme to convert into ice loss the elevation changes extracted from the sequential DEM at the locations of UAF laser measurements. These “laser simulated” ice losses ($\Delta V_{\text{SIMU-LASER}}$) are given in Table S4.

For seven out of 10 glaciers, Arendt *et al.*² report the ice loss for two time periods: the early period Δt_{early} “1950s-1995” and the recent period Δt_{recent} “1995-2001” (with exact time interval varying for each glacier). Thus, for each of these seven glaciers, we construct a single “long term” estimate (called ΔV_{UAF} , Table S4), by time-weighting their ice loss during Δt_{early} and Δt_{recent} (assuming that the loss for Δt_{recent} are also valid after 2001, which is justified according to recent repeat measurements using laser altimetry³⁶).

The small differences between $\Delta V_{\text{SIMU-LASER}}$ and ΔV_{UAF} demonstrate that the sequential DEM analysis (our work) and the laser altimetry study² lead to similar ice losses when the sequential DEM is sampled at the locations of UAF laser measurements. The absolute difference is $0.18 \text{ km}^3 \text{ yr}^{-1}$ or 2.5%.

Since we used the same profile-to-glacier extrapolation scheme as Arendt *et al.*² and the same map series as Arendt *et al.*² to represent the ‘old’ glacier surface, this good agreement is a further confirmation that our recent topography (from satellite imagery) is well-calibrated and does not contain any systematic biases. This analysis also indicates that the differences between ΔV_{UAF} and ΔV_{DEM} (Table S4) are mainly due to differences in sampling (laser profiling vs. comprehensive DEM coverage, see also Figure S3).

The absolute difference between $\Delta V_{\text{SIMU-LASER}}$ and ΔV_{UAF} ($0.18 \text{ km}^3 \text{ yr}^{-1}$) in Table S3 provides an estimate of the uncertainties of the difference between both techniques for seven glaciers sampled at the same locations. This uncertainty includes the errors from: (i) different recent topographies (airborne laser vs. satellite DEMs); (ii) recent topographies that are not acquired at the end of the ablation season and; (iii) uncertainty in map dates. UAF made an extensive analysis to find the exact dates of the aerial photographs used to derive the map contour lines (A. Arendt, personal communication, 2009) whereas we simply trusted the dates provided on the map sheets.

Assuming that these seven glaciers of different types and sizes, distributed in different Alaskan mountain ranges and totaling 5090 km² are representative of the rest of measured Alaskan glaciers, we propagate this uncertainty to all Alaskan ice masses as follow:

- (i) applied the same uncertainty to all Alaskan glaciers surveyed with sequential DEM (73% of the total Alaskan ice-covered area). The resulting uncertainty is $\pm 2.23 \text{ km}^3 \text{ yr}^{-1}$.
- (ii) doubled those uncertainties for unsurveyed ice-covered areas (27%) to take into account the additional uncertainties associated with regional extrapolation. The resulting uncertainty is $\pm 1.62 \text{ km}^3 \text{ yr}^{-1}$.
- (iii) multiplied our total ice loss by the difference (2.4%) in glaciated areas between glacier inventories used in Arendt *et al.*² and this study. This leads to an additional uncertainty of $\pm 1.00 \text{ km}^3 \text{ yr}^{-1}$.

Summing (i), (ii) and (iii), we compute the total uncertainty in the difference between methods. Our revised ice loss is thus $20.8 \pm 4.8 \text{ km}^3 \text{ yr}^{-1}$ w.e. lower than the laser altimetry ice loss.

Supplementary references

31. Adalgeirsdottir, G., Echelmeyer, K.A. & Harrison, W.D. Elevation and volume changes on the Harding Icefield, Alaska. *J Glaciol* **44**, 570-582 (1998).
32. Bretherton, C.S., Widmann, M., Dymnikov, V.P., Wallace, J.M. & Blade, I. The effective number of spatial degrees of freedom of a time-varying field. *J Climate* **12**, 1990-2009 (1999).
33. Beedle, M.J. et al. Improving estimation of glacier volume change: a GLIMS case study of Bering Glacier System, Alaska. *The Cryosphere* **2**, 33-51 (2008).
34. Cox, L.H. & March, R.S. Comparison of geodetic and glaciological mass-balance techniques, Gulkana Glacier, Alaska, USA. *J Glaciol* **50**, 363-370 (2004).
35. Larsen, C.F., Motyka, R.J., Freymueller, J.T., Echelmeyer, K.A. & Ivins, E.R. Rapid viscoelastic uplift in southeast Alaska caused by post-Little Ice Age glacial retreat. *Earth Planet Sc Lett* **237**, 548-560 (2005).
36. Larsen, C.F., Echelmeyer, K.A., Harrison, W.D., Arendt, A.A. & Lingle, C.S. Is Glacier wastage continuing to accelerate in NW North America? *Eos Trans. AGU* **89**(2008).